"W-shaped" volume curve with gated myocardial perfusion single photon emission computed tomography

Tokuo Kasai, E. Gordon DePuey and Irwin Sponder

Division of Nuclear Medicine, Department of Radiology, St. Luke's-Roosevelt Hospital Center,
Columbia University College of Physicians and Surgeons, New York, USA

Objectives: Gating errors (GEs) with ECG gated myocardial SPECT (G-SPECT) may occur irrespective of the presence or absence of arrhythmias. We evaluated the impact of GEs on both reconstructed tomograms and left ventricular ejection fraction (LVEF) derived from G-SPECT, and searched for clues to identify these errors. ***Methods:*** We studied 2 GE patients, 10 normal subjects (NLs), and 10 atrial fibrillation patients. Stress technetium-99m sestamibi G-SPECT was performed. Left ventricular (LV) contraction was evaluated in the beating slices. LVEF was calculated with G-SPECT using QGS (Cedars-Sinai, Los Angels) and p-FAST (Sapporo Medical University, Japan), and compared with that obtained by echocardiography (ECHO). LV volume curves were created by QGS and p-FAST. The heart rates (HRs) were calculated from the acquired images, and compared with their resting HRs. The mean count density of the myocardium was measured and time-activity curves were created. ***Results:*** In patients with GEs, bi-phasic LV contraction was demonstrated with fading-out towards end-diastole. G-SPECT underestimated LVEF compared to ECHO by 10% or more. The volume curves appeared "W-shaped." The HRs from the images were slower than the resting HRs. The count density decrement from frame #1 to #8 was larger than that of NLs. The time-activity curves were different in shape from those of NLs. ***Conclusions:*** G-SPECT underestimates LVEF in patients with GEs. These errors can be identified with a combination of visual inspection of beating slices, time-volume curves, and time-activity curves. Monitoring the HR is a clue for anticipating and avoiding these errors.

Key words: gating errors, myocardial SPECT, left ventricular function, volume curve, time-activity curve

INTRODUCTION

Left ventricular (LV) function can now be evaluated with ECG gated myocardial SPECT (G-SPECT), which has improved diagnostic accuracy for ischemia[1] and has afforded incremental prognostic value.[2] However, gating errors may render images suboptimal.[3] Moreover, both LV ejection fraction and wall motion may be neither accurate nor reliable. The etiology of these errors is multifold. Although gating errors may be anticipated and can be recognized easily by visual estimation in patients with arrhythmias such as atrial fibrillation,[4,5] they also occurs in the absence of arrhythmias, especially when the voltage of the R wave is relatively small compared to the T wave.[3] We observed two cases with additional types of gating error, where the ECG sensed not only R waves but also T waves, or where only every other R wave was sensed. The purpose of this study was to evaluate the impact of such GEs on both tomograms and LV function derived from G-SPECT, and search for clues to identify and anticipate these errors.

MATERIALS AND METHODS

Patient Population
We reviewed 1,687 consecutive G-SPECT studies in 2001 and 1,547 patients who showed normal sinus rhythm.
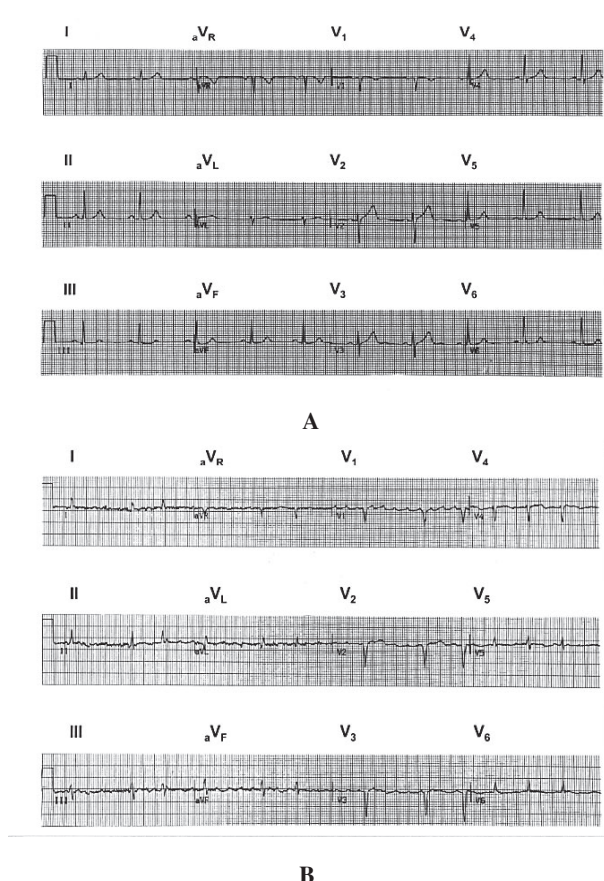
Fig. 1 Baseline 12-lead electrocardiograms. A (Case #1), Nomal ECG. B (Case #2), Atrial fibrillation with low voltage of QRS complex. QS patterns in V_1–V_3 are consistent with anteroseptal myocardial infarction.

Two patients with gating errors were identified whose volume curves appeared "W-shaped." We enrolled these 2 patients and also 10 normal subjects (NLs) and 10 atrial fibrillation patients (AFs) for comparison.

The criteria for NLs were defined as follows: 1. Low likelihood of coronary artery disease (<15%) based on age, gender, and the type of chest pain.[6] 2. Normal baseline ECG and definitely normal stress ECG results with no chest pain under appropriate stress achievement. 3. Definitely normal G-SPECT results based on both perfusion and functions. NLs were identified when all these 3 conditions were fulfilled.

Gated SPECT Acquisition and Processing
After intravenous administration of 855 MBq (two-day stress/rest protocol for case #1) or 1,147 MBq (single-day rest/stress protocol for case #2) of technetium-99m sestamibi (MIBI) during stress, ECG gated tomographic imaging of the heart was performed using 8-frame gating either 15 minutes after exercise, or 40 minutes after pharmacological stress. Either conventional treadmill exercise using the Bruce protocol or dipyridamole infusion (0.14 mg/kg over 4 minutes) was employed as the
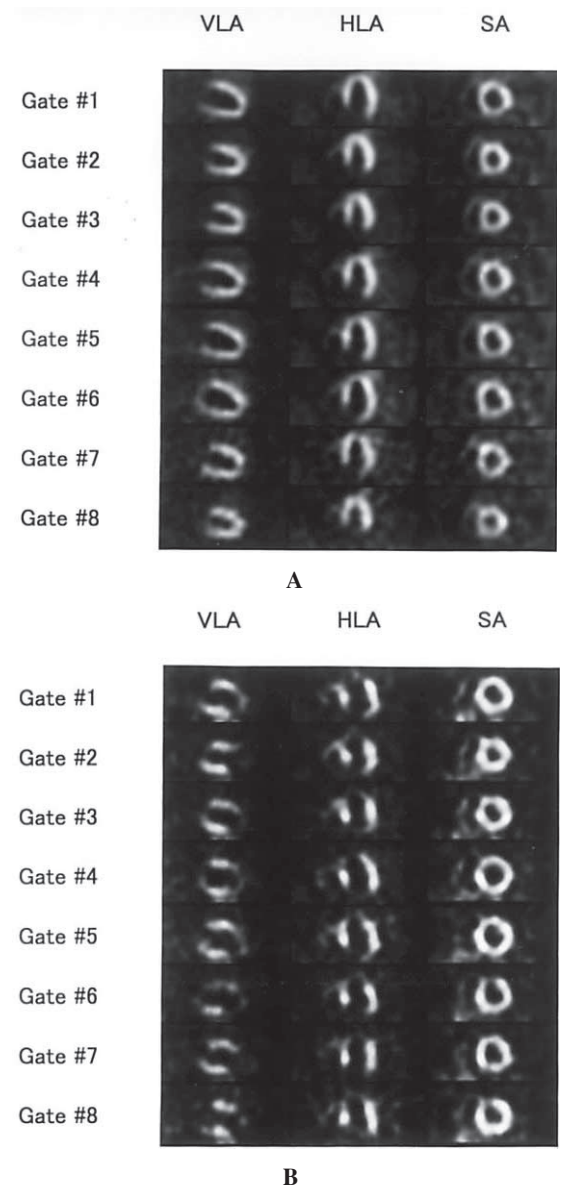

Fig. 2 Myocardial gated SPECT slices at stress. Bi-phasic contractions were observed in the beating slices. The images "faded out" towards end-diastole (A, Case #1; B, Case #2).

stress protocol.

The tomographic images were acquired with a rotating dual headed gamma camera (Optima or MG; GE Medical Systems, Israel) equipped with low energy, high resolution, parallel-hole collimators over 180 degrees in 32 (× 2) steps in a 64 × 64 matrix. All acquired data were processed with CEqual software on the GEnie system (GE Medical Systems, Israel) and transaxial tomograms were reconstructed using filtered backprojection with Ramp/ Butterworth filters (cutoff = 0.40 of Nyquist frequency, power = 10). Vertical long-axis, horizontal long-axis, and short-axis tomograms were derived from the transaxial images. The acceptance window for gated acquisition as a function of "Bad Beat Rejection" was set with the
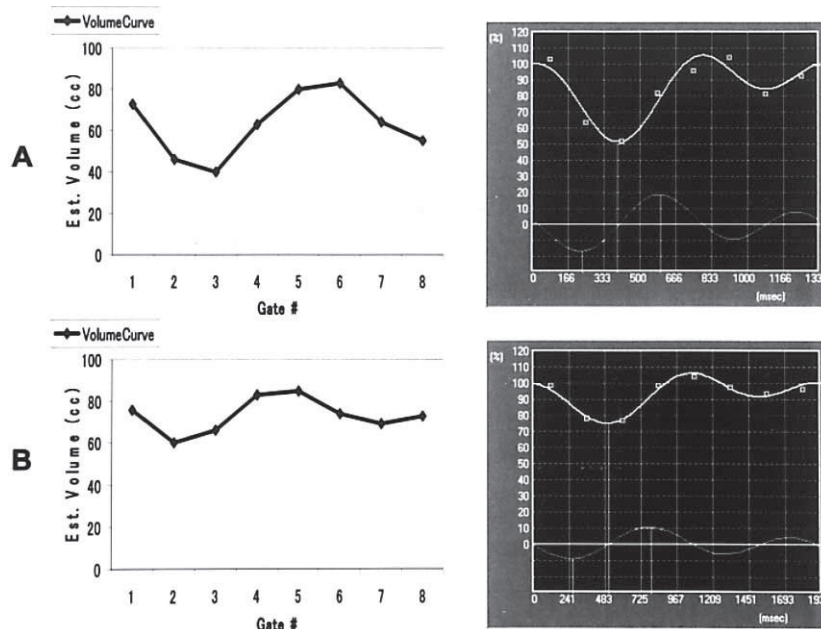
Fig. 3 The time-volume curves of the left ventricle obtained using QGS (*left*) and p-FAST (*right*). "W-shapes" were observed (A, Case #1; B, Case #2).

width of 150% (± 75%) around the average cardiac cycle (= "cardiac cycle") to eliminate both shorter and longer cycle beats due to arrhythmias. Neither attenuation nor scatter correction was performed. No patient motion or additional arrhythmias were detected in any of the patients or normal control subjects enrolled.

LV Functional Analysis
Visual assessment of LV contraction was accomplished by viewing gated tomographic slices in endless loop cinematic format. Reconstructed gated short axis slices were processed with both QGS and p-FAST. LVEFs were calculated by means of fully automated analysis with QGS, and manually modified analysis with p-FAST. LVEF was also assessed by 2-dimensional echocardiography, using a modified Simpson's method in patients with gating errors and compared with those calculated from G-SPECT. LV volume curves were created by both QGS and p-FAST.

Heart Rate Comparison
The average heart rates were calculated from the acquired images based on the time intervals between consecutive gated frames, and compared with the resting heart rates on the baseline ECG.

Count Density and Time-Activity Curve of Myocardium
The short-axis slices at the papillary muscle level of each gated frame were selected, and both epicardial and endocardial boundaries were delineated manually as the region of interest (ROI) for the measurement of the count density of the myocardium. The mean count densities of

the myocardium were calculated and plotted against the gated frames. This plot was regarded as the time-activity curve. The count density decrement from frame #1 to #8 was calculated.

Statistics
Data were expressed as the mean ± 1SD. We used one-way analysis of variance to test for overall differences in LVEF among the modalities, followed by Dunne correction for multiple comparisons. Statistical significance was considered to be indicated by $p < 0.05$. Analyses were performed using SPSS for Windows (version 10, SPSS Inc., Chicago, Illinois).

RESULTS

Case 1
A 54-year-old man who had no risk factors for coronary artery disease and no history of heart disease was referred for myocardial perfusion imaging because of typical anginal chest pain. His height and body weight were 158 cm and 63 kg, respectively. He exercised on the treadmill for 9 minutes 29 seconds, and achieved a peak heart rate of 154 bpm, which was 93% of his predicted maximal heart rate. He experienced no chest pain, and there were no ST segment changes or arrhythmias during exercise. Both the baseline ECG (Fig. 1A) and myocardial perfusion on the SPECT were normal; however, the beating slices revealed bi-phasic contraction, also with fading-out towards end-diastole (Fig. 2A). LVEF was calculated as 52% by QGS and 51% by p-FAST, whereas it was estimated to be 62% by echocardiography. LV volume
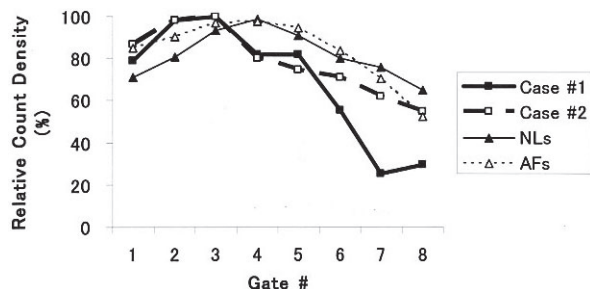
Fig. 4 The time-activity curves of the left ventricle. With Case #1, the curve demonstrated dual peaks, resembling an inverted "W-shape." The count density of the myocardium decreased rapidly after frame #5. In Case #2, a single peak was demonstrated. The count density of the myocardium decreased rapidly between frame #3 and #4, and thereafter decreased gradually.
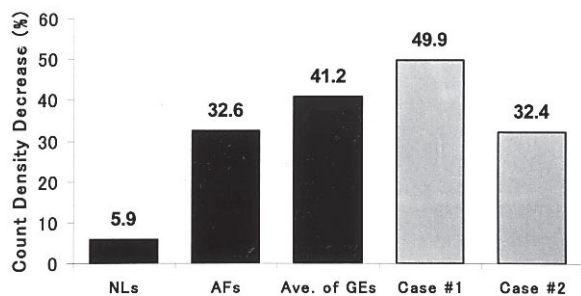

Fig. 5 The count density decrement from Frame #1 to #8. The magnitude of the count density decrease seemed to correlate with the degree of "fading-out" of the images towards end-diastole. The mean count density decrement from Gate #1 to #8 for the two GE patients was larger than that for NLs. Ave. = average.

curves appeared "W-shaped" (Fig. 3A). End-diastolic volume (EDV) and End-systolic volume (ESV) were 84.6 m*l* and 40.7 m*l* by QGS, respectively. The volumes of gated frame #5 and #6 exceeded that of frame #1. The HR was calculated as 45 bpm from the images, whereas the resting HR was 58 bpm. The count density of the myocardium rapidly decreased after frame #5 (Fig. 4). The count density decrement from frame #1 to #8 was 49.9% (Fig. 5). There were no "flickers" in the rotating projection images.

Case 2
An 85-year-old female who was hypertensive and had a history of prior myocardial infarction and heart failure was referred for myocardial perfusion imaging to assess residual ischemia after a recent myocardial infarction. Her height and body weight were 157 cm and 71 kg. On day 4 after admission the patient underwent pharmacologic stress myocardial perfusion SPECT. The baseline ECG showed atrial fibrillation and a QS pattern in V_1–V_3. Variable voltage of the R waves was noted (Fig. 1B). There was a very marked and extensive fixed perfusion defect throughout the distal half of the LV on perfusion

SPECT. The beating slices revealed apical akinesis. Additionally a bi-phasic pattern of contraction was present. The gated images also "faded-out" towards end-diastole to a lesser degree than in Case #1 (Fig. 2B). LVEF was calculated as 29% by QGS and 25% by p-FAST, whereas it was estimated to be 40% by echocardiography performed 3 days before. LV volume curves also appeared "W-shaped" (Fig. 3B). EDV and ESV were 85.5 m*l* and 60.7 m*l* by QGS, respectively. The volumes of gated frame #4 and #5 exceeded that of frame #1. The HR was calculated as 31 bpm from the images, whereas the resting HR was 71 bpm. The count density of the myocardium rapidly decreased between frame #3 and #4 and thereafter gradually decreased (Fig. 4). The count density decrement from frame #1 to #8 was 32.4% (Fig. 5). Frequent and severe "flickers" in the rotating projection images were demonstrated.

Time-Activity Curves
Both NLs and AFs revealed a relatively smooth transition throughout the time-volume curves with a single peak consistent with end-systole, whereas the two GE cases demonstrated "jagged" time-activity curves (Fig. 4). Case #1 demonstrated dual peaks, which implies that two end-systoles were present in the "cardiac cycle." The mean count density decrement from frame #1 to #8 with these two GEs patients was slightly greater than that of AF patients and obviously larger than that of NLs (GEs = 41.2 ± 12.4%; AFs = 32.6 ± 14.4%, p = NS; NLs = 5.9 ± 4.3%, p = 0.001, respectively) (Fig. 5).

DISCUSSION

The impact of gating errors due to arrhythmias has been reported.[4,5] Even if there are no arrhythmias, low R wave voltage may cause decreased trigger sensitivity, resulting in gating errors.[3] In Case #1, neither arrhythmias nor decreased voltage of the R wave was detected. However, bi-phasic contraction was demonstrated, which produce a "W-shaped" volume curve. The calculated HR from the images (45 bpm) was not close to 1/2 of the resting HR (58 bpm). The cardiac cycle length converted from the calculated HR (45 bpm   1,333 msec) was actually rather close to the interval between the initial R wave of the first cycle and T wave of the next cycle (1,320 msec). This implies that gating began at the first R wave and ended at the T wave of the next cycle. The volume curve by QGS successfully demonstrated this time-volume relationship showing 1 1/2 of a cycle rather than a complete "W-shape." However, this pattern was not demonstrated by p-FAST. The different algorithms for myocardial edge detection for these two programs might have affected the resultant volume curves.[7,8] Additionally, p-FAST employs Fourier transforms to delineate the volume curve to compensate for poor temporal resolution with G-SPECT.[8] This compensation might have contributed to the distor-
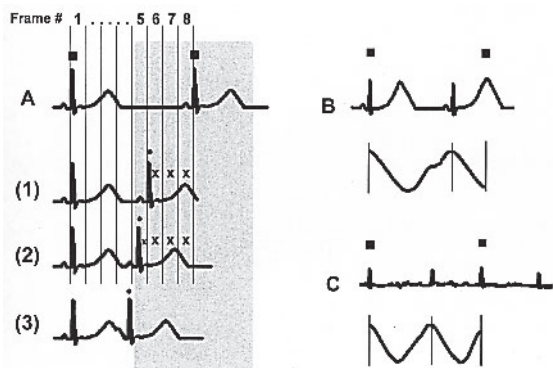
Fig. 6 A, The acceptance window and the 8 frames per R-R interval were set for gating. ▪ indicates trigger mark and the gray square indicates the acceptance window for Gating. Frame #6, 7, 8 ((1), (2)) and the second 1/2 of the frame #5 (2) do not include any data (indicated by "X") because acquisition should be stopped at the second R wave (•). This mechanism leads to the "fading-out" phenomenon. The shorter (or longer) cycle length beat would not be registered when the second R wave (•) falls outside of the acceptance window, causing "flicker" (3). B and C, Schematic representation of the altered sensing for gating. Both competitive voltages between the R wave and the T wave (B) and variable, and low voltage of the R wave (C) lead to altered sensing for gating.

tion of the volume curve.

In Case #2, bi-phasic contraction and a "W-shaped" volume curve were also demonstrated. The calculated HR from the images (31 bpm) was close to 1/2 of the mean resting HR (71 bpm). This implies that the "cardiac cycle" set for gating included two entire cardiac cycles and that only every other R wave was sensed. In Case #1, the voltage was so competitive between the R wave and T wave that the relative difference in voltage between these two waves might have varied during acquisition, causing altered trigger sensitivity. In Case #2, the voltage of the R wave varied, which also altered trigger sensitivity. Therefore, we assumed that this altered trigger sensitivity occurs with either variable voltage of the R wave (like in Case #2) or when the R wave voltage is low and similar to the T wave (like in Case #1).

LVEFs calculated by both QGS and p-FAST underestimated those determined by echocardiography by 10% or more. The relatively small size of LV might have contributed in part to this underestimation, especially for QGS.[9,10] Even though atrial fibrillation was demonstrated in Case #2, LVEF should have been minimally affected by this arrhythmia.[4,5] Therefore, in Case #2 rather than atrial fibrillation being the main cause of underestimation of LVEF, we assume that the culprit factor was incorrect definition of the cardiac cycle (only 8 data points per two entire cardiac cycles). Thus, LVEF and LV volumes tend to be greatly affected by incorrect definition of the cardiac cycle as exemplified by the two cases presented in this report. In both cases, this phenomenon was manifested by

the shorter HR (bpm) calculated from the images than the resting HR. Accordingly, LVEF will be consistently underestimated in this manner if the HR set for gating is smaller than the actual one.

The count density decrement from frame #1 to #8 seemed to be proportional to the degree of fading-out of images towards end-diastole. This assumption was supported by the difference of the degree of fading-out of images between Case #1 and #2. The "fading-out" phenomenon is a manifestation of the variability of the HR during acquisition. The same phenomenon has been reported with equilibrium radionuclide angiography.[11] With varying "HRs," some cardiac cycles fall outside the acceptance window for bad beat rejection and are rejected, contributing to an overall decrease in count density. Such variability in HR also leads to "flicker" in the rotating projection images. With shorter cycle length within the acceptance window, the fixed time duration set for each gated frame results in the frames after the second R wave being empty. This suggests that with increasing acceptance of short cycles, the greater will be the degree of fading-out towards end-diastole (Fig. 6). The degree of fading-out of images thus depends on both the number of the registered short cycle beats and also the shortness of their cycle length.

Araujo et al. reported that soft tissue attenuation artifacts are most evident in low count density studies and obese patients with dense soft tissue, such as abdominal protuberance and prominent breasts. Therefore these attenuation artifacts tend no appear in the right coronary artery territory in men and the left descending coronary artery territory in women.[12] The count density decrement from frame #1 to #8 seemed to be affected by soft tissue attenuation in part because the rest of the frames are relatively low count density images. However, Case #2 did not show higher count density decrement compared with Case #1 in spite of obesity. Thus, the body habitus may affect the count density decrement to a lesser degree compared to the number of rejected cardiac cycles due to gating errors by means of the function of bad beat rejection.

Reverse redistribution (i.e. washout) phenomenon of technetium-99m sestamibi has attracted a great deal of attention in terms of viability in acute myocardial infarction,[13,14] vasospasm,[15] chronic coronary artery disease,[16] and heart failure.[17] However, once "flicker" or fading-out of images is observed, a considerable number of cardiac cycles will be rejected, resulting in a declined count density study. Therefore, these types of gating error spoil the usefulness of washout rate evaluation, unless the rejected cardiac cycles are combined with the registered cardiac cycles to calculate the washout rate.

Although "W-shaped" volume curves may be noticed by visual inspection of the beating images in one cardiac cycle, bi-phasic contraction would often remain unrecognized and be regarded as normal contraction in the

cinematic loop display because first and second contractions tend to be regarded as identical unless the volume curve is verified. In fact, in the present two cases incorrect LVEF and no gating errors were reported initially. The cinematic loop display is prevalent for assessing wall motion. Therefore, we should make every effort to avoid these errors. One should confirm that the trigger for gating is appropriate before starting the acquisition of a gated study. Once these errors are involved, we should pay more attention to LV contraction patterns and keep in mind these errors to avoid misinterpretation of gated SPECT studies.

CONCLUSIONS

Gating errors with "W-shaped" volume curves are subtle and difficult to recognize but nevertheless result in significant underestimation of LVEF. These errors can be identified by careful visual inspection of beating slices, time-volume curves, and time-activity curves. Moreover, monitoring the HR before and during the gated acquisition may also be helpful in anticipating and avoiding these errors.

ACKNOWLEDGMENTS

REFERENCES

1. Bavelaar-Croon CD, Atsma DE, van der Wall EE, et al. The additional value of gated SPECT myocardial perfusion imaging in patients with known and suspected coronary artery disease. *Nucl Med Commun* 2001; 22: 45–55.
2. Sharir T, Germano G, Kavanagh PB, et al. Incremental prognostic value of post-stress left ventricular ejection fraction and volume by gated myocardial perfusion single photon emission computed tomography. *Circulation* 1999; 100: 1035–1042.
3. Kasai T, DePuey EG, Shah AA, et al. Impact of Gating Errors with ECG Gated Myocardial Perfusion SPECT. *J Nucl Cardiol* 2003; 10: 709–711.
4. Nichols K, Dorbala S, DePuey EG, et al. Influence of arrhythmias on gated SPECT myocardial perfusion and function quantification. *J Nucl Med* 1999; 40: 924–934.
5. Nichols K, Yao SS, Kamran M, Faber TL, Cooke CD, DePuey EG. Clinical impact of arrhythmias on gated SPECT cardiac myocardial perfusion and function assessment. *J Nucl Cardiol* 2001; 8: 19–30.
6. Diamond GA, Forrester JS. Analysis of probability as an aid in the clinical diagnosis of coronary artery disease. *N Engl J Med* 1979; 300: 1350–1358.
7. Germano G, Kiat H, Kavanagh PB, et al. Automatic quantification of ejection fraction from gated myocardial perfusion SPECT. *J Nucl Med* 1995; 36: 2138–2147.
8. Nakata T, Katagiri Y, Odawara Y, et al. Two- and three-dimensional assessment of myocardial perfusion and function by using technetium-99m sestamibi gated SPECT with a combination of count- and image-based techniques. *J Nucl Cardiol* 2000; 7: 623–632.
9. Feng B, Sitek A, Gullberg GT. Calculation of the left ventricular ejection fraction without edge detection: application to small hearts. *J Nucl Med* 2002; 43: 786–794.
10. Toba M, Kumita S, Cho K, Mizumura S, Kijima T, Nakajo H, et al. Comparison of Emory and Cedars-Sinai methods for assessment of left ventricular function from gated myocardial perfusion SPECT in patients with a small heart. *Ann Nucl Med* 2000; 14: 421–426.
11. DePuey EG. Evaluation of cardiac function with radionuclides. In: Gottschalk A, Hoffer PB, Potchen EJ eds. *Diagnostic Nuclear Medicine, 2nd ed.* Baltimore; Williams & Wilkins, 1988: 355–398.
12. Araujo W, DePuey EG, Kamran M, et al. Artifactual reverse distribution pattern in myocardial perfusion SPECT with technetium-99m sestamibi. *J Nucl Cardiol* 2000; 7: 633–638.
13. Fujiwara S, Takeishi Y, Hirono O, et al. Reverse redistribution of ^{99m}Tc-sestamibi after direct percutaneous transluminal coronary angioplasty in acute myocardial infarction: relationship with wall motion and functional response to dobutamine stimulation. *Nucl Med Commun* 2001; 22: 1223–1230.
14. Takeishi Y, Sukekawa H, Fujiwara S, et al. Reverse redistribution of technetium-99m-sestamibi following direct PTCA in acute myocardial infarction. *J Nucl Med* 1996; 37: 1289–1294.
15. Ono S, Takeishi Y, Yamaguchi H, Abe S, Tachibana H, Sato T, et al. Enhanced regional washout of technetium-99m-sestamibi in patients with coronary spastic angina. *Ann Nucl Med* 2003; 17: 393–398.
16. Richter WS, Cordes M, Calder D, et al. Washout and redistribution between immediate and two-hour myocardial images using technetium-99m sestamibi. *Eur J Nucl Med* 1995; 22: 49–55.
17. Kumita S, Seino Y, Cho K, Nakajo H, Toba M, Fukushima Y, et al. Assessment of myocardial washout of Tc-99m-sestamibi in patients with chronic heart failure: comparison with normal control. *Ann Nucl Med* 2002; 16: 237–242.